A New Atomistic Simulation Scenario for Assessing Solvents for Polymers and Application to Thermoresponse of Poly(N-isopropylacrylamide) in Water

Edder J. García, Debdip Bhandary, Martin T. Horsch, and Hans Hasse*

Laboratory of Engineering Thermodynamics (LTD), University of Kaiserslautern, Erwin-Schrödinger-Str. 44, 67663 Kaiserslautern, Germany.

*Email: edder.garcia-manzano@mv.uni-kl.de

Keywords: thermoresponsive polymers, hydrogels, smart polymers, umbrella sampling, potential of mean force, molecular dynamics simulations.

Abstract

Studying equilibrium states of polymers in solution by atomistic simulations is a challenging task as the available computation time is often not sufficient to ensure representative sampling of the phase space. One approach to tackle this problem is to create a simulation scenario which is simple enough to enable adequate sampling of equilibrium states but retains essential parts of the physics of the polymer in solution. We present such a scenario here. It aims at assessing the quality of solvents for polymers by atomistic equilibrium simulations. Two periodic polymer molecules are studied in the explicit solvent. The centers of mass of the polymer molecules are restrained such that both move in a collision plane. The distance *d* between these centers lends itself as order parameter so that advanced sampling techniques like umbrella sampling can be applied easily. Both a state corresponding to dissolved polymers (large *d*) and a state corresponding to aggregated polymers (small *d*) can be defined, and many transitions between both states can be observed in reasonable simulation time. The scenario misses the intramolecular collapse of the single chain, but it retains full atomistic detail regarding the polymer-solvent and the intermolecular polymer-polymer interactions. The latter also reflect some aspects of the intramolecular collapse. The simple scenario gives a good indication whether for a given force field and a given temperature the polymer will be dissolved or not in equilibrium. The thermoresponsive behavior of PNIPAM in water is studied as a showcase.

1. Introduction

Polymer solutions occur in many technical and natural processes. It is a fundamental to know whether a given polymer will dissolve in a given solvent at given temperature and pressure. Using atomistic simulations for predicting this is attractive. Furthermore, atomistic simulations yield insight in the nature of the phenomena which lead to the macroscopic behavior of the solutions.

The results of atomistic simulations depend on the force field that is used for describing the particle interactions. In the following, it is assumed that the force field is given. We acknowledge that suitable force fields for describing thermodynamic properties of polymer solutions are often not available, but show that the new simulation scenario developed here can contribute to mitigating this shortage.

But also for a given force field, the prediction of equilibrium properties of polymer solutions by atomistic simulations is a formidable task. In a first step, a simulation scenario has to be chosen. This is far from trivial. The most realistic scenario is one in which many polymer chains move freely in the solvent, and the number of polymer chains and solvent molecules is chosen in such a way that they match the macroscopic polymer concentration. Even for moderately large polymer chains, this typically leads to a prohibitively large phase space that cannot be sampled adequately by atomistic simulations due to limitations of computational power.

There are different ways to tackle this problem: (a) brute force simulations with very large simulation times[1,2], (b) advanced sampling techniques[3,4], (c) coarse-graining of the polymer[5], (d) implicit or coarse-grained solvents[6,7]. In the present work, we aim at exploiting the high potential of all-atom or united-atom force fields so that only (a) and (b) are considered. Unfortunately, even when (a) and (b) are fully exploited and suitably combined, it may still be impossible to sample the phase space reliably for the scenario described above. Hence, the problem has to be addressed from the side of the scenario. The most common simplified scenario one for studying the quality of polymer solvents is to use only a single polymer chain and to observe whether it collapses or not. Obviously, in this scenario, only intermolecular polymer-polymer interactions are considered in this scenario while the intramolecular polymer-polymer interactions are entirely neglected. Unfortunately also this simplified scenario suffers from the same problems as the more realistic scenario discussed above, i.e., the phase space often turns out to be too large to be sampled reliably. A more detailed discussion of this is given at the end of this section for NIPAM polymer chains. The simulation problems encountered in these studies of NIPAM

motivated the present work, in which a new simple scenario for studying the quality of polymer solvents by atomistic equilibrium simulations was developed.

In the new scenario, two periodic polymer molecules are used which span from one side of the simulation box to the side vis-à-vis. The arrangement is such that no intramolecular collapse occurs and the center of mass of the polymers stays close to the backbone. The centers of the polymer molecules are furthermore restrained in such a way that both move within a common collision plane. This drastically reduces the phase space which has to be sampled so that studies of equilibria become feasible. Furthermore, the distance d between the centers of the two polymer chains lends itself as order parameter so that advanced sampling techniques like umbrella sampling can be applied readily. They enable calculations of the free energy of the system as a function of d. Both a state corresponding to the dissolved polymer (large numbers of d) and a state corresponding to aggregated polymers (small numbers of d) can be defined easily, and many transitions between both states are observed in feasible simulation times so that the free energy difference between both states can be determined reliably.

We acknowledge that this scenario is a bold simplification. It misses the intramolecular collapse of the single polymer chain. However, this is not more or less bold than using a single polymer chain and neglecting the intermolecular aggregation. However, the latter has the disadvantage, that it does not solve the sampling problem. The present two-chain scenario retains full atomistic detail regarding the polymer-solvent and the intermolecular polymer-polymer interactions. The latter also reflect some aspects of the intramolecular collapse, for instance, the rearrangement of the side chains upon polymer-polymer contact.

We claim that this simple scenario gives a good indication whether for a given force field the polymer will be dissolved or not in equilibrium. No strict proof of this claim can be given, but the usefulness of the scenario can be demonstrated, see below.

Furthermore, some theoretical arguments support the claim. In the following, the change of the free energy of the system upon a transition between the aggregated state and the one in which the individual polymer chains are dissolved is considered. The new scenario retains atomistic resolution regarding all relevant interactions (polymer-solvent, solvent-solvent, and polymer-polymer). Hence, the enthalpic contributions are reasonably covered by the new scenario. There is more concern about the entropic contributions because in the new scenario the intermolecular collapse is hindered. However, the new scenario also captures the influence of the polymer's solvent shell and the release of solvent molecules from that shell upon aggregation. It is well known that this is the main part of the entropic contribution in many situations. The part of the entropic contributions which is neglected here is that related to the conformation change of the polymer chain, which is e.g., also neglected in Flory's theory.

As a showcase for demonstrating the usefulness of the new scenario, the thermo-responsive behavior of poly(N-isopropylacrylamide) (PNIPAM) in water was studied. Thermoresponsive polymers abruptly change a physical property in response to variations in the temperature. Over the past decades, thermoresponsive polymers have been the subject of intense research due to their potential application in drug delivery, tissue engineering, biosensors, etc.[8–10] The most widely studied thermoresponsive polymers is PNIPAM. It has a lower critical solution temperature (LCST) in water of 305 K[11–13], i.e., above that temperature PNIPAM and water show a liquid-liquid phase split, i.e., water is a

good solvent for PNIPAM at low temperatures, but a poor solvent at high temperatures. In many cases, PNIPAM is used as a hydrogel, in which the polymer chains are cross-linked. Cross-linking does not change the thermoresponsive behavior of PNIPAM substantially.[11] Below the LCST, the hydrogel is swollen and retains a significant amount of water, above the LCTS the hydrogel is collapsed, and the water is released. On the molecular scale, the process involves a transition of PNIPAM chains from an extended coil conformation to a compact globule conformation.[13–15]

Molecular dynamics (MD) simulations with all-atom or united atom models have played an important role in understanding the thermoresponsive behavior of PNIPAM.[11,16–21] The most common scenario used in these studies is the simulation of a single 30mer-N-isopropylacrylamide (30mer-NIPAM) chain in explicit water.[11,22,23] However, with reasonable computational effort, this scenario can be presently only be studied for a few hundred nanoseconds. It has become clear recently that this does not enable a sufficient sampling of the phase space so that no reliable information on the equilibrium state as a function of temperature can be obtained. [1,2] In previous work, our group has used this approach for studying the thermoresponsive behavior of PNIPAM in water.[11,16] We show in Appendix A that also these simulations were not long enough to yield reliable information on the equilibrium. The unsatisfactory sampling in simulations of the single oligomer scenario has two main reasons: First, atomistic MD simulations use a time step of the order of femtoseconds while conformational transformations of large molecules occur on the scale of milliseconds.[24] This is confirmed for PNIPAM by an experimental study in which the relaxation time to obtain a thermodynamically stable globule state chain from a coiled state is found to be of the order of milliseconds.[25,26] There is a gap of three to four orders of magnitude between that time scale and that which is presently accessible by direct

simulations. Second, the usual simulation scenario only relies on intramolecular collapse. Thus, the simulation time required to observe the coil-to-globule transition is limited by the by the rearrangement of many internal degrees of freedom. Thereby, the oligomer must overcome conformational energy barriers which cause a complex energy landscape with many local minima in which the simulation can get trapped.

The present scenario focusses on intermolecular collapse. It is known from experiments that intermolecular collapse of PNIPAM plays an important role in thermoresponsive behavior in both dilute and concentrated solutions.[13,27] It is known from dynamic and static light scattering that even in diluted solution, during a heating cycle PNIPAM chains undergo first a contraction, however without fully collapsing, before intermolecular collapse leads to the globule state.[13] Recently, by using small-angle neutron scattering, it has been found that the collapse of PNIPAM is driven by chain-chain interaction, while the radius of gyration of single molecules decreases only slightly.[27] A pure intramolecular collapse of PNIPAM can only be observed in extremely diluted solutions (< 5 μg/mL).[25,28–30]

In the following, first, the two-chain simulation scenario is presented, then its application to studying the thermoresponsive behavior of PNIPAM in water is discussed. The force field for the PNIPAM + water system as well as the simulation set up for that application are specified. The two-chain simulation scenario is used in two ways in these studies: First, direct molecular dynamics (MD) simulations are carried out. It is shown that, despite the simplicity of the new scenario, it is difficult to obtain reliable information on the equilibrium from such direct simulations. This strongly underpins the statement that there is no hope to retrieve such information from scenarios which have a much larger phase space, like the that in which a 30mer-NIPAM chain moves freely in water. To overcome this problem, the fact is used that the two-chain scenario has a natural order parameter, the

distance d between the polymer chains. The distance d characterizes the transition path from the aggregated to the dissolved state. Umbrella sampling was applied for calculating the Potential of Mean Force (PMF) along that transition path, which is feasible with acceptable computational effort. PMF profiles $G(d)$ were determined for PNIPAM in water at temperatures between 280 and 360 K using the OPLS/AA + SPC/E force field with standard mixing rules, as it has been applied in several previous studies, including our own[11,16,32]. Contrarily to earlier statements in the literature[11], it is shown here that this force field yields demixing of PNIPAM and water in the entire studied temperature range, i.e., no lower critical solution temperature LCST is found. This supports a recent statement of Leonhard and co-workers[32] obtained using direct simulations of single NIPAM chains.

For completeness, it is shown that an LCST can be obtained by a simple modification of the mixing rule. Upon a slight increase of the polymer-solvent dispersive interaction energy, an LCST is found in the region in which it is also found in experiments. Also, the enthalpy change observed upon demixing is reasonably well predicted. This indicates that the two-chain scenario is useful for predicting the behavior of polymer-solvent systems also in other situations. It could, e.g., be used for predicting co-nonsolvency.

2. Two-chain Scenario

The two-chain simulation scenario is set up as follows. In a first step, two chains of the studied polymer consisting of N monomer units each are relaxed in vacuum. In the present work, N = 15 was chosen. The minimal chain length is limited by the cutoff radius r_c. To avoid spurious interactions between periodic images, the chain length has to exceed $2\,r_c$. The two chains are inserted in a rectangular simulation box with their backbones parallel to the z-axis. The box length in z-direction l_z is chosen such that it equals the length of the

relaxed chains, so that the chains span from one side of the box to the side vis-à-vis, see Figure 1 and periodic boundaries are used so that the chains cannot collapse during the simulation as long as l_z is not changed. Information on the choice of the other two box lengths l_x, l_y is given below. After the insertion of the two polymer chains, the simulation box is filled with the pre-equilibrated water.

To further reduce the configuration space the movement of the polymer chains in the box is restrained such that their centers of mass move in a collision plane. That plane is marked red in Figure 1 and is perpendicular to the *y*-axis. Technically, a harmonic potential is applied to the *y*-component of the vector connecting the centers of mass of both chains such that the *y*-component of the inter-chain distance *d* fluctuates around zero. The collision plane itself can move in the *y*-direction in the simulation box when both chains move together in that direction. But the two chains can move independently and freely in both the *x*- and the *z*-direction.

The distance *d* between the centers of mass of the chains is a natural order parameter for the present simulation scenario. It is dominated by the distance in *x*-direction whereas in the other two directions only small fluctuations occur. Those in the *z*-direction are not taken into account in the calculation of the distance, i.e., *d* measures the distance in the *x*,*y*-plane. An “aggregated state” and a “dissolved state” of the polymer chains are defined by two threshold values: for $d < d^*$ the polymer chains are considered to be aggregated, for $d > d^{**}$ they are considered to be dissolved. States with *d* between these thresholds belong to the transition region. Choosing numbers for d^* and d^{**} is somewhat arbitrary, but can be based on physical arguments which depend on the nature of the polymer and the polymer-polymer interactions. Simple geometrical arguments can be used like considering the length

of side chains of the polymer, but the choice can also be based on information obtained in the simulation run, e.g., on certain site-site radial distribution functions or the potential of mean force G(*d*), as discussed below.

The simulation box size l_x is chosen to be somewhat larger than d^{**} to enable sampling of the dissolved state. The box length l_y must be large enough to avoid direct interactions between the polymer chain and its solvent shell with its periodic image.

The system containing the two polymer chains and the solvent is equilibrated first in the NVT-ensemble and then in the NPT-ensemble. The NPT-ensemble is also used for the production run to avoid the pressure fluctuations in the NVT ensemble. Since periodic molecules are bonded across the simulation box, isotropic pressure coupling fails to rescale the box dimensions. Therefore, semi-isotropic pressure coupling has to be employed. This may lead to a collapse of the simulation box, i.e. to a decrease of l_z below 2 r_c. The simplest way to avoid this would be to use a barostat which keeps the box length l_z constant. However, this method would give a poor control of the pressure in the plane that is perpendicular to the z-axis. Therefore, a simple workaround was used, which is described in the Supporting Information.

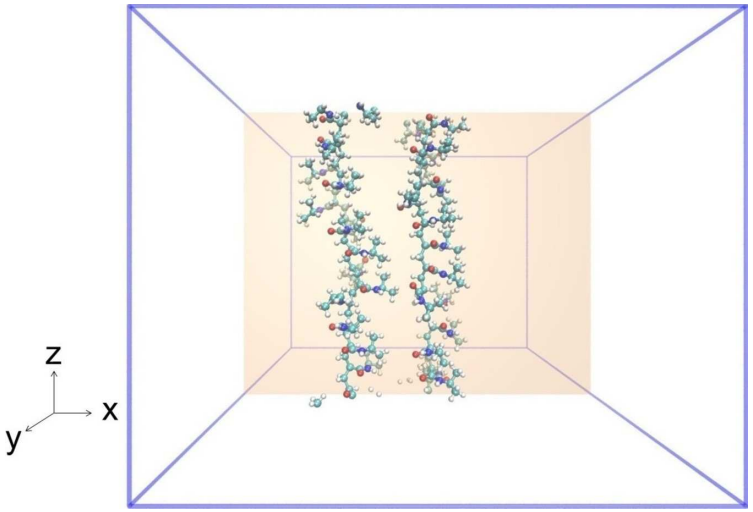

Figure 1. Two-chain simulation scenario illustrated by a snapshot of a simulation of PNIPAM in water. Water molecules are not shown for clarity. The semitransparent red surface indicates the collision plane to which the centers of mass of both PNIPAM molecules are restrained. The plane can move backward and forward in the direction of the *y*-axis. Carbons are depicted in green, oxygens in red, nitrogens in blue, and hydrogens in white.

3. Application to PNIPAM + Water

3.1 *Force field*

PNIPAM molecules were modeled by the OPLS/AA[31] force field, and water molecules by the SPC/E[32] model, as suggested previously.[11] The PNIPAM molecules used in this work are syndiotactic. The model parameters are given in the Supporting Information.

A modified Berthelot mixing rule was applied to calculate the polymer-water LJ energy parameters (ε_{pw}),

$$\varepsilon_{pw} = \xi \sqrt{\varepsilon_{pp}\varepsilon_{ww}} \quad (1)$$

where ξ is a state-independent parameter, which can be employed to adjust the interactions between the LJ sites of the polymer (p) and water (w). First, ξ was set to 1 to evaluate the unmodified force field as it was used in Ref. [11], and then it was increased to 1.10 to favor polymer-water interactions. The last value was obtained from preliminary tests. The primary goal of this modification is not to reproduce the experimental LCST of PNIPAM accurately, but merely to demonstrate the capability of the two-chain simulation scenario to describe such phenomena.

According to the recommendations for the OPLS/AA force field, a geometric-mean mixing rule is also used for the LJ size parameters describing the interactions between LJ sites of the polymer and water

$$\sigma_{pw} = \sqrt{\sigma_{pp}\sigma_{ww}} \quad . \quad (2)$$

For the polymer-polymer interaction, unmodified geometric-mean mixing rules were applied to determine mixed Lennard-Jones parameters.

3.2 Simulations

The simulation scenario is that described in Section 2. All simulations were performed with Gromacs 5.0.[33] Two types of simulations were carried out: direct MD simulations and MD simulations with umbrella sampling.

Two PNIPAM chains of 15 monomers were used, leading to an initial simulation box length in the z-direction of l_z = 3.785 nm, as described in Appendix B. In the other dimensions, the initial simulation box lengths are l_x = 5.0 nm, l_y = 5.0 nm. The resulting number of water molecules in the box is 2883. For an illustration, see Figure 1. Results from a systematic study of the effect of the number of monomers per chain and the initial size of the box in the *x* and *y*-direction are presented in the Supporting Information. The force constant of the harmonic potential which is used to keep the two polymer chains in the collision plane was set to 7000 kJ mol^{-1} nm^{-2} based on results from preliminary studies. The threshold values for the order parameter were chosen to be d^* = 1.2 nm and d^{**} = 2.2 nm. The cut-off radius was 1.4 nm. The length of the side chains of PNIPAM is about 0.4 nm. Hence, a rough estimate indicates that for d > (0.4 + 0.4 + 1.4) nm = 2.2. nm there are no polymer-polymer interactions. In fact, the simulation results show that these interactions are already very weak at distinctly smaller numbers of d. Using the same type of argument, we deduce that the backbones interact for d < 1.4 nm, so that for $d < d^*$ = 1.2 nm there are strong interactions not only between the side chains but also between the backbones. These choices of d^* and d^{**} are also confirmed by the results for the potential of mean force $G(d)$ presented below.

The system is equilibrated in the canonical (NVT) ensemble for 100 ps, followed by 250 ps equilibration and 120 ns sampling in the NPT ensemble. Simulations were carried out for temperatures between 280 to 360 K in intervals of 20 K. The pressure was always 1 bar.

Semitropic coupling was used to keep the pressure constant. As a result, the size of the box in the *z*-direction can change independently of that in the *x*- and *y*-direction. The intermolecular collapse was avoided by applying restraints on specific atoms in the backbone of the chains. Details are given in Appendix B.

3.3 PMF from umbrella sampling

The potential of mean force $G(d)$ is determined from the probability distribution function $P(d)$, which describes the probability of finding the system in states in an infinitesimal interval around d. As direct simulations are impracticable for converging $P(d)$ (see below), umbrella sampling[34–36] was applied. In umbrella sampling, the system is restrained in successive configurations, called umbrella windows, along the transition path. Thus, favorable and unfavorable states on the transition path can be satisfactorily sampled. A harmonic potential $W(d)$ was applied to restrain the system to specific sections of the path. The relation between the biased probability distribution $P^b(d)$ and $G(d)$ is given by

$$G(d) = -RT \ln P^b(d) - W(d) + G_0 \tag{3}$$

where G_0 is used for normalization. $G(d)$ was obtained here using 34 overlapping windows in which d was varied between 0.8 and 2.2 nm. The weighted histogram analysis method WHAM[37] was used to reconstruct $G(d)$ along the path as implemented in Gromacs.[38] The normalization was chosen so that G = 0 for the maximal distance d = 2.2 nm. Technical details of the simulations and calculation of the PMF are given in Appendix C.

3.4 Results and discussion

3.4.1 Direct simulations (unmodified polymer-water mixing rule, ξ =1)

Two independent simulations with different initial configurations, an aggregated state (d_{ini} = 0.9 nm) and a dissolved state (d_{ini} = 1.8 nm), were conducted at 280 K using the two-chain scenario. The results are shown in Figure 3. For both simulations, the polymer-polymer distance d fluctuates between 0.86 and 2.5 nm. The upper limit of d results from the size of the simulation box in the x-direction (~5 nm) and the periodic boundary conditions while the lower limit results from polymer-polymer repulsion. For the simulation with d_{ini} = 0.9 nm, the PNIPAM chains remain aggregated until approximately t = 16 ns, after this time they move into the dissolved state for 5 ns. Then, the chains recover the aggregated state again and stay in this configuration for the rest of the simulation time of 120 ns. For the simulation with d_{ini} = 1.8 nm, a significant fluctuation in the polymer-polymer distance is observed. During the initial 100 ns, the PNIPAM chains are mainly in the dissolved state, but several collisions with d < 1.4 nm occur approximately every 10 ns before the molecules aggregate permanently at t = 94 ns. Movies of both simulations (V1 and V2) are supplied with the Supporting Information. Even though there seems to be a preference for the aggregated state at the studied conditions, the results are ambiguous: the simulation with d_{ini} = 0.9 nm remained most of the time in the dissolved state whereas the simulation d_{ini} = 1.8 nm stayed most of the time in the aggregated state.

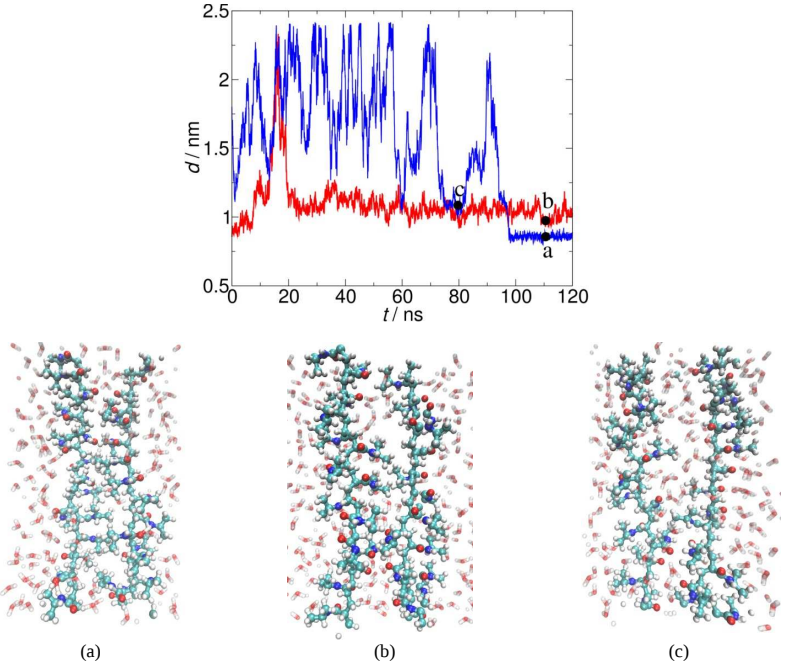

Figure 2. Simulation results for PINPAM in water at 280 K obtained with the two-chain scenario (ξ = 1.0). Top: chain-chain distance as a function of simulation time at 280 K. The simulations were started in different configurations: d_{ini} = 0.9 nm (red line) and d_{ini} = 1.8 nm (blue line). Bottom: Snapshots of favorable conformations: (a) fully aggregated (d = 0.87 nm); (b) partially aggregated (d = 0.96 nm), and (c) water-mediated aggregation (d = 1.12 nm). Only water molecules in the layer of 1 nm around PNIPAM chains are depicted.

Two different aggregated states are attained at the end of the simulation runs, which both seem to be favorable: one with d = 0.87 nm and the other with d = 0.96 nm, cf. Error: Reference source not found. Snapshots of corresponding configurations are shown in the bottom of Figure 2. For d = 0.87 nm (Panel a, fully aggregated state) most of the side chains are in direct contact with the side chains of the other PNIPAM molecule, whereas for d = 0.96 nm (Panel b, partially aggregated state) there are fewer side-chain side-chain contacts. Furthermore, Figure 3 shows that there is a third particularly favorable state with d = 1.12 nm which corresponds to a water-mediated aggregation (Panel c).

The transition between the aggregated and the dissolved state can be observed in both directions within a reasonable simulation time. In the traditional single-oligomer scenario, generally not more than one transition is obtained for similar simulation time (see Supporting Information), and a much larger simulation volume is needed.[2,11] Still, even with the two-chain scenario, it is difficult to obtain unambiguous results regarding the equilibrium, when direct simulations are applied, cf. Figure 3.

3.4.2 Umbrella sampling (unmodified polymer-water mixing rule, ξ =1)

The two-chain simulation scenario was used to determine the potential of mean force $G(d)$ by umbrella sampling as described above. The results for ξ = 1 and 280 K are presented in Figure 3. They show that the free energy barrier that has to be overcome for the transition from the dissociated to the aggregated state is only about 2 kJ/mol and therefore of the order of RT. Despite this comparatively small thermodynamic barrier in the two-chain simulation scenario, it takes almost 100 ns for that transition to happen in direct

simulations (Error: Reference source not found), which shows that there are important kinetic limitations even in the simple scenario used here. On the other hand, the free energy barrier which has to be overcome for the transition from d = 0.92 nm to d = 2.20 nm, i.e., going from the aggregated state to the dissolved state, is about 14 kJ/mol, corresponding to about 6 RT. Together with the additional kinetic limitations, this explains why in direct simulations the disentanglement is hard to observe, even with the simple scenario.

The global minimum of $G(d)$ indicates the most stable conformation. At 280 K, the global minimum of $G(d)$ is at d = 0.92 nm (Figure 3), i.e., in an aggregated state. The potential of mean force was also determined for 300, 320, 340, and 360 K. The results are presented in the Supporting Information. They show that the tendency of PNIPAM to aggregate increases with increasing the temperature, in accordance with the experimental data. Therefore, it can be concluded that the OPLS/AA + SPC/E force field is unable to reproduce the temperature-dependent transition of the PNIPAM equilibrium configuration. Recently, a similar conclusion was reported based on simulations of the phase transition of short oligomers.[2]

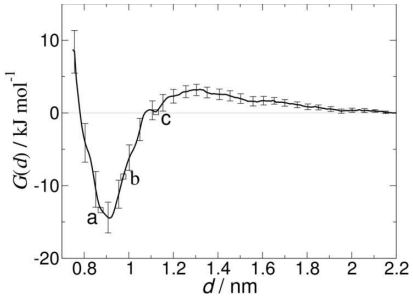

Figure 3. Potential of mean force of the transition between the dissolved and the aggregated state of PINPAM in water at 280 K. Results obtained with the two-chain scenario using umbrella sampling (ξ = 1). The points a - c correspond to favorable configurations observed in the direct simulation shown in Figure 2: (a) fully-aggregated, (b) partially aggregated, and (c) water-mediated. The error bars were obtained from the simulation runs in the individual windows.

The direct simulations generally do not lead to the global minimum in the PMF. The favorable conformations found in the direct simulations described in Section 3.4.1 (aggregation: full, partial, water-mediated, cf. Error: Reference source not found) are plotted in Figure 3 by indicating the respective values of d. Neither of these conformations corresponds to the global minimum of the PMF, so they are all metastable conformations. However, it can be seen that conformation (a) is close to the global minimum.

3.4.3 Umbrella sampling (modified polymer-water mixing rule, ξ =1.1)

The results discussed above show that the unmodified OPLS + SPCE force field does not predict the temperature dependent transition of the PNIPAM equilibrium configuration at all studied temperatures the PNIPAM chains were found to be aggregated. To demonstrate the ability of the two-chain scenario to study the transition a modified force field was used, which was chosen based on results of a preliminary study: the polymer-water dispersion interaction was increased by 10 %, i.e., ξ = 1.10. Figure 4 shows results for the potential of mean force $G(d)$ obtained using ξ = 1.1 for temperatures between 280 and 360 K. Comparing $G(d)$ obtained for 280 K and ξ = 1.0 (Figure 3) and ξ = 1.1 (Figure 4), it can be seen that increasing ξ leads to an important increase in $G(d)$ for all values of d. For ξ = 1.1 and 280 K, $G(d)$ still has a minimum of around d = 0.9 nm, but that minimum is no longer the global minimum. The global minimum is now the dissolved state obtained for a larger distance d. At 280 K and ξ = 1.1 (Figure 4), the energy barrier which has to be overcome for the transition from the metastable aggregated state at about d = 0.9 nm to the stable dissolved state at large d is about 3 RT.

Increasing the temperature shifts the global minimum in the potential of mean force $G(d)$. For all studied temperatures, there is a minimum of $G(d)$ at about d = 0.9 nm, corresponding to an aggregated state. But only for temperatures above about 300 K, that minimum is the global minimum, i.e., the equilibrium configuration changes from dissolved to aggregated at about 300 K, as observed in experiments. At 300 K, $G(d)$ has two minima in which $G(d)$ is close to zero, and the system fluctuates between these two states, hindered by a thermodynamic barrier of about 3 RT.

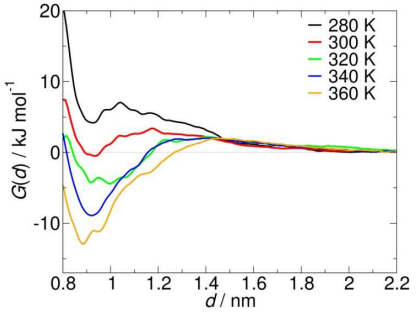

Figure 4. Potential of mean force of the transition between the dissolved and the aggregated state of PINPAM in water for different temperatures. Results obtained with the two-chain scenario using umbrella sampling (ξ = 1.1).

The Gibbs energy of the dissolved state G_d is zero by definition here. The Gibbs energy of the aggregated state G_a can be obtained from an integration of G(d) by[39]:

$$G_a = -RT \ln \frac{\int_{d_1}^{d_2} \exp\left[\frac{G(d)}{RT}\right] dd}{d_2 - d_1} \qquad (4)$$

The upper bound used in the present work for the calculation of G_a is $d_2 = d^* = 1.2$ nm. As no configurations were observed below 0.8 nm, d_1 is set to 0.8 nm. As G_d is zero, the number for G_a is also the number obtained for the change of the Gibbs energy upon the transition $\Delta G_{d\to a}$. The results for $\Delta G_{d\to a}$ obtained from the evaluation of the potentials of mean force $G(d)$ for the different temperatures are shown in Figure 5. The error bar reported for $\Delta G_{d\to a}$ is the difference obtained from the integration in Equation 4 when using

$G(d)$ and $G(d) + \Delta G(d)$, respectively, where the uncertainty of the potential of mean force $\Delta G(d)$ was estimated using the bootstrap analysis (see Appendix C for details).

It can be seen that $\Delta G_{d\to a}$ changes its sign at about 300 K, as it also is expected from Figure 4. Figure 5 also shows the results from a fit of $\Delta G_{d\to a}$ with:

$$\Delta G_{d\to a} = \Delta H_{d\to a} - T\,\Delta S_{d\to a} \qquad (5)$$

from which the changes of the enthalpy $\Delta H_{d\to a}$ and the entropy $\Delta S_{d\to a}$ per monomer unit of PNIPAM and the transition temperature T_θ, at which $\Delta G_{d\to a}$ changes its sign, was determined. The resulting number for T_θ = 309 ± 9 K is in good agreement with the experimental data for the LCST of PNIPAM, cf. Table 1. The same holds for $\Delta H_{d\to a}$ and $\Delta S_{d\to a}$ for which the experimental values scatter considerably. The uncertainty of the simulated values reported in Table 1 were obtained by fitting ($\Delta G_{c\to g}$ + $\Delta\Delta G_{c\to g}$) vs. T, where the uncertainty $\Delta\Delta G_{c\to g}$ was taken from the results shown in Figure 5.

The result for the transition temperature T_θ depends strongly on the choice of ξ. Therefore, additional simulations were therefore carried out ξ = 1.15, which yielded T_θ = 339 ± 14 K. For details see Supporting Information.

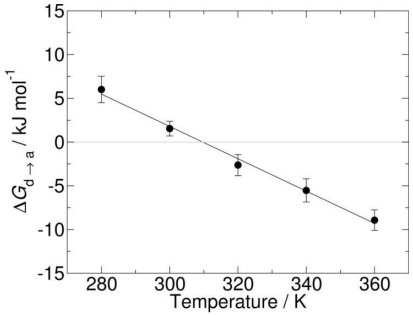

Figure 5. Free energy change of the transition from the dissolved to the aggregated state of PINPAM in water as a function of temperature. Results obtained with the two-chain scenario using umbrella sampling (ξ = 1.1).

Table 1. Thermodynamic properties of the transition from the dissolved to the aggregated state of PINPAM in water. Comparison of simulation results obtained with the two-chain scenario using umbrella sampling to experimental data from the literature. The binary interaction coefficient used in the simulations is ξ = 1.1.

Property	Simulation	Experiment
T_θ / K	309 ± 9	305[a]-306[b]-307[c]-310[d]
$\Delta H_{c\to g}$ kJ/mol per monomer	1.9 ± 0.1	1.8[b]-3.8[c]-4.4[d]-4.8[e]
$\Delta S_{c\to g}$ / J/K/mol per monomer	6.3 ± 0.1	6[b]-12[c]-14[d]

[a] Swelling of the hydrogel, from Ref. [11].

[b] DSC of a 20mer-PNIPAM, from Ref. [40].

[c] DSC of a 92mer-PNIPAM, from Ref. [41].

[d] DSC of PNIPAM with a molar mass of 4.9 x 10^4 g/mol, from Ref. [42].

[e] DSC of PNIPAM with a molar mass of 3.3 x 10^3 g/mol, from Ref [43].

4. Conclusions

In this work, a two-chain molecular simulation scenario is presented which can be used for assessing the quality of solvents for polymers based on atomistic force fields. In the scenario, the intermolecular collapse of two periodic polymer chains is monitored.

In atomistic studies of polymer solutions, often scenarios are used in which a single, freely moving oligomer is monitored, which is so long that it can undergo intramolecular collapse. Unfortunately, the phase space of such scenarios is often so large that reliable information on the equilibrium cannot be obtained in acceptable simulation time. E.g., once the single oligomer is collapsed, it is usually impossible to observe its unfolding in the simulation. The sampling problems increase when multiple freely moving chains are used. Hence, for practical reasons, it is hard to assess the quality of solvents of polymers using atomistic force fields with the established molecular simulation methods. The new scenario aims at solving this problem by reducing the phase space which has to be sampled in such a way that essential elements of the atomistic description of the transition of the polymer from the dissolved state to the aggregated state in the solvent are preserved. All interactions are accounted for with atomistic resolution. The only compromise which is made is that intramolecular collapse is excluded. This leads to a significant reduction of the phase space

so that equilibria can now be monitored. Despite the simplification, essential elements of the intermolecular collapse are retained: the release of solvent molecular from the polymer's solvent shell, the increased number of polymer-polymer contacts, etc. Basically only the entropic contribution of the folding is neglected. Compared to other simplifications, e.g., deficiencies of existing force fields, this is considered to be acceptable here.

In the new two-chain scenario the distance of the two polymer chains d is a natural order parameter so that it is particularly suited for applications of advanced sampling techniques which facilitate the calculation of the potential of mean force $G(d)$ from which global and local equilibrium states and energy barriers between these states can be found.

The usefulness of the two-chain scenario is demonstrated using the thermoresponsive behavior of PINPAM in water as an example. The potential of mean force profiles reveals that the OPLS/AA + SPC/E force field predicts that water is a bad solvent for all studied temperature which were between 280 and 360 K. Therefore, the binary interaction coefficient ξ in the modified mixing rule for the water-polymer interaction was increased from 1 to 1.1. Using this modified force field, it was demonstrated that the thermo-responsive behavior of PINPAM in water is described well: water is a good solvent at low temperatures and a bad one at high temperatures. The transition temperature T_θ as well as the enthalpy and entropy change per monomer unit of PINPAM were found to be in good agreement with experimental data. This supports the statement that the simplifications of the scenario are acceptable from a practical standpoint.

The new scenario opens the route for assessing the quality of different solvents or for different polymers based solely on atomistic force fields. This includes mixed solvents,

solvents containing salts, copolymers, polyelectrolytes, etc. The success or failure of such predictions strongly depends on the force field. The new two-chain scenario also enables improving the force fields for describing polymer-solvent systems.

Appendix A. Criticism of Walter *et al.* [11]

The paper of Walter *et al.* [11] reports experimental and molecular simulation results on the coil-to-globule transition of PNIPAM in water. The molecular simulations were carried out using the single chain scenario with 30mer PINIPAM. The length of the production run was 20 - 40ns. It is shown in the Supporting Information that this is far too short to sample the equilibrium reliably. The simulation time was extended here to 120 ns, but still, no adequate sampling was obtained, see Supporting Information. It is known from the literature, that the sampling problems persist even when the simulation time is increased to about 1000 ns.[1] A second problem with the simulations of Walter *et al.* [11] is that the simulation volume was not large enough to avoid artificial head-tail interactions in some orientations of the stretched chain. This artificially favors the stretched state over the collapsed state.

Appendix B. MD simulations details

The system was equilibrated by the following protocol. First, PNIPAM chains were relaxed in vacuum and then with the solvent, using the steepest descent method with a

target force of 100 kJ mol^{-1} nm^{-2}. The initial inter-chain distance d_{ini} was kept at the desired value during the equilibrations steps using a harmonic potential.

In the simulations, the leapfrog integrator was used with a time step of 1 fs. Non-bonded interactions were truncated using a cutoff radius of 1.4 nm. Tail corrections were implemented for the potential energy and pressure. The neighbor list was updated every ten integration steps. Electrostatic interactions were calculated by the PME method.[44] The grid spacing was fixed at 0.12 nm, and the extrapolation order was carried out up to fourth. The cutoff radius for the real space sum was set to 1.4 nm. Periodic boundary conditions were applied in all dimensions of space. The temperature was established by the V-scaling thermostat[45] with a time coupling constant of 0.1 ps. The Berendsen barostat was used to set the pressure.[46] The pressure coupling constant was 0.5 ps and the compressibility 4.5 10^{-5} bar^{-1}. Semi-isotropic pressure coupling was employed. The *z*-lattice vector of the box was adjusted independently of the *x* and *y*-vectors. Resulting from the action of the barostat, the simulation box could collapse in the *z*-direction as a consequence of the intramolecular collapse of the PNIPAM chains. The intermolecular collapse was avoided by restraining the distance between specific pairs of methylene carbons (-CH_2-) in the backbone. Specifically, a harmonic potential was applied when the distance between the methylene carbons was lower than the distance in the pre-equilibrated linear configuration. Thus, the harmonic potential only pulls to avoid the intermolecular collapse, but it does not prevent the stretching. Three restraints pairs per chain were applied to allow certain flexibility of the chain. The restrained pairs were the methylene carbons in monomers 1-7, 4-10, and 9-15. The force constant for the harmonic potential was 20000 kJ mol^{1} nm^{-2}. These constraints are work-arounds which facilitate the NPT simulation with the given barostat. They have no modeling background.

Appendix C. Umbrella sampling and calculation of the potential of mean force

Umbrella sampling was carried out for the two-chain simulation scenario for a distance d between 0.8 and 2.2 nm. A total of 34 umbrella windows were used. For d > 1.1 nm, the central position of the window is on a grid with a spacing of 0.05 nm. For d < 1.1 nm, the grid spacing was 0.025 nm.

The force constant of the harmonic potential for restraining d was 7000 kJ mol^{-1} nm^{-2}. This value was obtained by trial and error. Two factors were considered to get the force constant: maximizing the overlap of umbrella histograms of successive windows while keeping a reasonable number of windows.[47] As an example, an umbrella histogram is shown in the Supporting Information.

The equilibration and production simulations were carried as follows. First, the pull algorithm in Gromacs was applied to generate the initial configuration for a given d.[33] Then, for each window, two successive equilibration simulations were conducted: the first one in the NVT ensemble for 100 ps, and the second in the NPT ensemble for 750 ps. The same simulation conditions and parameters as described in Appendix B were applied. After equilibration, the production simulation in the NPT ensemble was conducted. Short independent simulations in narrow umbrella windows reduce statistical errors and increase computational efficiency.[47] The independent simulations also avoid the system getting trapped in a given configuration, which is critical in sampling the aggregated state. Thus, for each umbrella window, eight independent production simulations of 3 ns each were conducted, so the total production time per window was 24 ns. Since 34 windows were defined, the total simulation time used to determine each PMF profile was 816 ns.

In production runs, the mean force was recorded every 10 fs. The potential of mean force $G(d)$ was calculated along d by using the WHAM in Gromacs.[38] The reference state of the

PMF was taken at 2.2 nm, which correspond to the dissolved state. To determine the uncertainty of the PMF profiles, we used the bootstrap method[38] with 200 bootstraps. The PMF was calculated using a running average and did not change after 15 ns per window (for details see Supporting Information).

Nomenclature

Symbols

d	distance
$G(d)$	potential of mean force
P	probability distribution
T	absolute temperature

Abbreviations

DSC	differential scanning calorimetry
OPLS/AA	optimized potentials for liquid simulations / all-atom
PMF	potential of mean force
PNIPAM	Poly(N-isopropylacrylamide)
SPC/E	extended simple point charge (water model)

Subscripts

a	aggregated state
d	dissolved state
ini	initial

Acknowledgment

The authors thank Juan M. Castillo, Jonathan Walter, and Jadran Vrabec for fruitful discussions. The authors acknowledge financial support from the Reinhart Koselleck

Program (HA1993/15-1) of the German Research Foundation (DFG) and the German Federal Ministry of Education and Research (BMBF) within the project TalPas (01IH16008F). The present work was conducted under the auspices of the Boltzmann-Zuse Society of Computational Molecular Engineering (BZS), and the simulations were carried out on Elwe at the Regional University Computing Center Kaiserslautern (RHRK) under the grant TUKL-TLMV, on SuperMUC at the Leibniz Supercomputing Center (LRZ), Garching, under the grant SPARLAMPE (pr48te), and on Hazel Hen at the High Performace Computing Center, Stuttgart (HLRS), under the grant MMHBF2.

References

(1) Kang, Y.; Joo, H.; Kim, J. S. Collapse–Swelling Transitions of a Thermoresponsive, Single Poly(N-Isopropylacrylamide) Chain in Water. *J. Phys. Chem. B* **2016**, *120* (51), 13184–13192.
(2) Boţan, V.; Ustach, V.; Faller, R.; Leonhard, K. Direct Phase Equilibrium Simulations of NIPAM Oligomers in Water. *J. Phys. Chem. B* **2016**, *120* (13), 3434–3440.
(3) Day, R.; Paschek, D.; Garcia, A. E. Microsecond Simulations of the Folding/unfolding Thermodynamics of the Trp-Cage Miniprotein. *Proteins Struct. Funct. Bioinforma.* **2010**, *78* (8), 1889–1899.
(4) Galbraith, M. L.; Madura, J. D. Identifying Trends in Hydration Behavior for Modifications to the Hydrophobicity of Poly(n-Isopropylacrylamide). *J. Mol. Graph. Model.* **2017**, *78*, 168–175.
(5) Abbott, L. J.; Stevens, M. J. A Temperature-Dependent Coarse-Grained Model for the Thermoresponsive Polymer poly(N-Isopropylacrylamide). *J. Chem. Phys.* **2015**, *143* (24), 244901.
(6) Schmid, A. J.; Dubbert, J.; Rudov, A. A.; Pedersen, J. S.; Lindner, P.; Karg, M.; Potemkin, I. I.; Richtering, W. Multi-Shell Hollow Nanogels with Responsive Shell Permeability. *Sci. Rep.* **2016**, *6*, 22736.
(7) Mukherji, D.; Kremer, K. Coil–Globule–Coil Transition of PNIPAm in Aqueous Methanol: Coupling All-Atom Simulations to Semi-Grand Canonical Coarse-Grained Reservoir. *Macromolecules* **2013**, *46* (22), 9158–9163.
(8) Ward, M. A.; Georgiou, T. K. Thermoresponsive Polymers for Biomedical Applications. *Polymers* **2011**, *3* (3), 1215–1242.
(9) Klouda, L. Thermoresponsive Hydrogels in Biomedical Applications: A Seven-Year Update. *Eur. J. Pharm. Biopharm. Off. J. Arbeitsgemeinschaft Für Pharm. Verfahrenstechnik EV* **2015**, *97* (Pt B), 338–349.
(10) Stuart, M. A. C.; Huck, W. T. S.; Genzer, J.; Müller, M.; Ober, C.; Stamm, M.; Sukhorukov, G. B.; Szleifer, I.; Tsukruk, V. V.; Urban, M.; Winnik, F.; Zauscher, S.; Luzinov, I.; Minko, S. Emerging Applications of Stimuli-Responsive Polymer Materials. *Nat. Mater.* **2010**, *9* (2), 101–113.
(11) Walter, J.; Ermatchkov, V.; Vrabec, J.; Hasse, H. Molecular Dynamics and Experimental Study of Conformation Change of poly(N-Isopropylacrylamide) Hydrogels in Water. *Fluid Phase Equilibria* **2010**, *296* (2), 164–172.
(12) Schild, H. G. Poly(N-Isopropylacrylamide): Experiment, Theory and Application. *Prog. Polym. Sci.* **1992**, *17* (2), 163–249.
(13) Cheng, H.; Shen, L.; Wu, C. LLS and FTIR Studies on the Hysteresis in Association and Dissociation of Poly(N-Isopropylacrylamide) Chains in Water. *Macromolecules* **2006**, *39* (6), 2325–2329.
(14) Tokuhiro, T.; Amiya, T.; Mamada, A.; Tanaka, T. NMR Study of poly(N-Isopropylacrylamide) Gels near Phase Transition. *Macromolecules* **1991**, *24* (10), 2936–2943.
(15) Zeng, F.; Tong, Z.; Feng, H. N.m.r. Investigation of Phase Separation in poly(N-Isopropyl Acrylamide)/water Solutions. *Polymer* **1997**, *38* (22), 5539–5544.
(16) Walter, J.; Sehrt, J.; Vrabec, J.; Hasse, H. Molecular Dynamics and Experimental Study of Conformation Change of poly(N-Isopropylacrylamide) Hydrogels in Mixtures of Water and Methanol. *J. Phys. Chem. B* **2012**, *116* (17), 5251–5259.
(17) Tamai, Y.; Tanaka, H.; Nakanishi, K. Molecular Dynamics Study of Polymer–water Interaction in Hydrogels. 1. Hydrogen-Bond Structure. *Macromolecules* **1996**, *29* (21), 6750–6760.
(18) Tamai, Y.; Tanaka, H.; Nakanishi, K. Molecular Dynamics Study of Polymer–water Interaction in Hydrogels. 2. Hydrogen-Bond Dynamics. *Macromolecules* **1996**, *29* (21), 6761–6769.
(19) Du, H.; Wickramasinghe, R.; Qian, X. Effects of Salt on the Lower Critical Solution Temperature of Poly (N-Isopropylacrylamide). *J. Phys. Chem. B* **2010**, *114* (49), 16594–16604.
(20) Du, H.; Wickramasinghe, S. R.; Qian, X. Specificity in Cationic Interaction with poly(N-Isopropylacrylamide). *J. Phys. Chem. B* **2013**, *117* (17), 5090–5101.
(21) Abbott, L. J.; Tucker, A. K.; Stevens, M. J. Single Chain Structure of a poly(N-Isopropylacrylamide) Surfactant in Water. *J. Phys. Chem. B* **2015**, *119* (9), 3837–3845.
(22) Tucker, A. K.; Stevens, M. J. Study of the Polymer Length Dependence of the Single Chain Transition Temperature in Syndiotactic Poly(N-Isopropylacrylamide) Oligomers in Water. *Macromolecules* **2012**, *45* (16), 6697–6703.
(23) Deshmukh, S. A.; Sankaranarayanan, S. K. R. S.; Suthar, K.; Mancini, D. C. Role of Solvation Dynamics and Local Ordering of Water in Inducing Conformational Transitions in poly(N-Isopropylacrylamide) Oligomers through the LCST. *J. Phys. Chem. B* **2012**, *116* (9), 2651–2663.
(24) Bolhuis, P. G.; Chandler, D.; Dellago, C.; Geissler, P. L. Transition Path Sampling: Throwing Ropes over Rough Mountain Passes, in the Dark. *Annu. Rev. Phys. Chem.* **2002**, *53*, 291–318.
(25) Xu, J.; Zhu, Z.; Luo, S.; Wu, C.; Liu, S. First Observation of Two-Stage Collapsing Kinetics of a Single Synthetic Polymer Chain. *Phys. Rev. Lett.* **2006**, *96* (2), 27802.
(26) Ye, X.; Lu, Y.; Shen, L.; Ding, Y.; Liu, S.; Zhang, G.; Wu, C. How Many Stages in the Coil-to-Globule Transition of Linear Homopolymer Chains in a Dilute Solution? *Macromolecules* **2007**, *40* (14), 4750–4752.
(27) Hammouda, B.; Jia, D.; Cheng, H. Single-Chain Conformation for Interacting Poly(N-Isopropylacrylamide) in Aqueous Solution. *Open Access J. Sci. Technol.* **2015**, *3*.
(28) Wu, C.; Zhou, S. Thermodynamically Stable Globule State of a Single Poly(N-Isopropylacrylamide) Chain in Water. *Macromolecules* **1995**, *28* (15), 5388–5390.
(29) Wu, C. A Comparison between the `Coil-to-Globule' Transition of Linear Chains and the "volume Phase Transition" of Spherical Microgels. *Polymer* **1998**, *39* (19), 4609–4619.

(30) Graziano, G. On the Temperature-Induced Coil to Globule Transition of Poly-N-Isopropylacrylamide in Dilute Aqueous Solutions. *Int. J. Biol. Macromol.* **2000**, *27* (1), 89–97.
(31) Jorgensen, W. L.; Maxwell, D. S.; Tirado-Rives, J. Development and Testing of the OPLS All-Atom Force Field on Conformational Energetics and Properties of Organic Liquids. *J. Am. Chem. Soc.* **1996**, *118* (45), 11225–11236.
(32) Berendsen, H. J. C.; Grigera, J. R.; Straatsma, T. P. The Missing Term in Effective Pair Potentials. *J. Phys. Chem.* **1987**, *91* (24), 6269–6271.
(33) Van Der Spoel, D.; Lindahl, E.; Hess, B.; Groenhof, G.; Mark, A. E.; Berendsen, H. J. C. GROMACS: Fast, Flexible, and Free. *J. Comput. Chem.* **2005**, *26* (16), 1701–1718.
(34) Patey, G. N.; Valleau, J. P. A Monte Carlo Method for Obtaining the Interionic Potential of Mean Force in Ionic Solution. *J. Chem. Phys.* **1975**, *63* (6), 2334–2339.
(35) Torrie, G. M.; Valleau, J. P. Nonphysical Sampling Distributions in Monte Carlo Free-Energy Estimation: Umbrella Sampling. *J. Comput. Phys.* **1977**, *23* (2), 187–199.
(36) Kästner, J. Umbrella Sampling. *Wiley Interdiscip. Rev. Comput. Mol. Sci.* **2011**, *1* (6), 932–942.
(37) Kumar, S.; Rosenberg, J. M.; Bouzida, D.; Swendsen, R. H.; Kollman, P. A. The Weighted Histogram Analysis Method for Free-Energy Calculations on Biomolecules. I. The Method. *J. Comput. Chem.* **1992**, *13* (8), 1011–1021.
(38) Hub, J. S.; de Groot, B. L.; van der Spoel, D. G_wham—a Free Weighted Histogram Analysis Implementation Including Robust Error and Autocorrelation Estimates. *J. Chem. Theory Comput.* **2010**, *6* (12), 3713–3720.
(39) Berendsen, H. J. C. *Simulating the Physical World: Hierarchical Modeling from Quantum Mechanics to Fluid Dynamics*; Cambridge University Press, 2007.
(40) Freitag, R.; Garret-Flaudy, F. Salt Effects on the Thermoprecipitation of Poly-(N-Isopropylacrylamide) Oligomers from Aqueous Solution. *Langmuir* **2002**, *18* (9), 3434–3440.
(41) Tiktopulo, E. I.; Uversky, V. N.; Lushchik, V. B.; Klenin, S. I.; Bychkova, V. E.; Ptitsyn, O. B. "Domain" Coil-Globule Transition in Homopolymers. *Macromolecules* **1995**, *28* (22), 7519–7524.
(42) Kunugi, S.; Tada, T.; Tanaka, N.; Yamamoto, K.; Akashi, M. Microcalorimetric Study of Aqueous Solution of a Thermoresponsive Polymer, poly(N-Vinylisobutyramide) (PNVIBA). *Polym. J.* **2002**, *34* (5), 383–388.
(43) Otake, K.; Inomata, H.; Konno, M.; Saito, S. Thermal Analysis of the Volume Phase Transition with N-Isopropylacrylamide Gels. *Macromolecules* **1990**, *23* (1), 283–289.
(44) Darden, T.; York, D.; Pedersen, L. Particle Mesh Ewald: An N·log(N) Method for Ewald Sums in Large Systems. *J. Chem. Phys.* **1993**, *98* (12), 10089–10092.
(45) Bussi, G.; Donadio, D.; Parrinello, M. Canonical Sampling through Velocity Rescaling. *J. Chem. Phys.* **2007**, *126* (1), 14101.
(46) Berendsen, H. J. C.; Postma, J. P. M.; Gunsteren, W. F. van; DiNola, A.; Haak, J. R. Molecular Dynamics with Coupling to an External Bath. *J. Chem. Phys.* **1984**, *81* (8), 3684–3690.
(47) Roux, B. The Calculation of the Potential of Mean Force Using Computer Simulations. *Comput. Phys. Commun.* **1995**, *91* (1), 275–282.

Abstract graphics

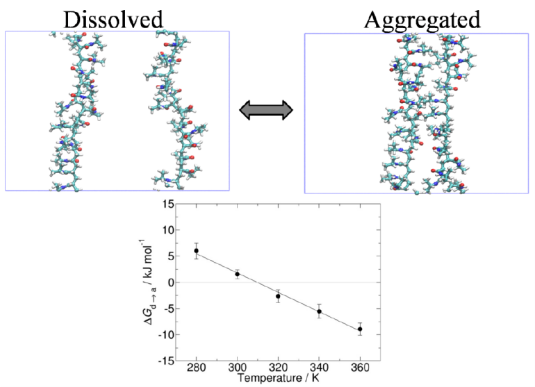

Supporting information

A New Atomistic Simulation Scenario for Assessing Solvents for Polymers and Application to Thermoresponse of Poly(N-isopropylacrylamide) in Water

Edder J. García, Debdip Bhandary, Martin Horsch, and Hans Hasse

Laboratory of Engineering Thermodynamics, University of Kaiserslautern, Erwin-Schrödinger-Str. 44, 67663 Kaiserslautern, Germany.

1. Criticism of Walter *et al.* [1]

In a recent paper from our group [1], the coil-to-globule transition of poly(N-isopropylacrylamide) (PNIPAM) in water was studied by experiments and molecular dynamics (MD) simulations. Direct MD simulations were carried out using a PNIPAM chain constructed of 30 monomeric units (30mer-PNIPAM) in water and production runs of 20-40 ns. The 30mer-PNIPAM chain was modeled with three force fields: Gromos-87 [2], GROMOS-96 53A6 [3,4], and OPLS-AA [5,6]; while for water two models were applied: SPC/E [7] and TIP4P [8]. The conclusion was that the OPLS-AA + SPC/E force field is able to predict the experimental conformational transition of PNIPAM qualitatively.

In follow-up work, we detected that the size of the simulation volume used in Ref. [1] was not large enough to always avoid that the head and the tail of the stretched 30mer-PNIPAM chain interact through the periodic boundary conditions. In Ref. [1], the size of the simulation volume was 9 nm × 7 nm× 7 nm. In a typical stretched state, the head-to-tail distance of a 30mer-PNIPAM chain, measured as the largest distance between two monomer segments in the backbone, is about 6 nm. Thus, with a cut-off radius of 1.5 nm, if the 30mer-PNIPAM chain is oriented parallel to the longest side of the volume, no head-tail interactions occur. However, as the polymer rotates, artificial head-tail interactions do play a role. This problem may have also occurred in similar works on PNIPAM carried out by other authors, e.g. [9–11].

Furthermore, the direct simulation method used in Ref. [1] is not suitable for adequately sampling the phase space of the 30mer-PNIPAM chain. Problems in direct simulations of PNIPAM chains in water have recently been reported by other authors [12]. To verify whether

direct MD simulation can be used to study the conformation transition of PNIPAM, we repeated the simulations of the 30mer-PNIPAM chain in water using a larger simulation volume and longer simulation times than those used in Ref. [1]. The convergence of the simulations was monitored by the corrected Gelman-Rubin test.[13] It shows that even these simulations do not allow for a statement on the equilibrium properties of the system.

MD simulations were carried out using the method described in Ref. [1]. A 30mer-PNIPAM chain was placed in the simulation volume aligned with the *x* axis. Two different sizes of the simulation volume were used. A small volume with dimensions of 9 nm × 7 nm × 7 nm (size in *x*, *y*, and *z* directions) containing 14469 water molecules, as in Ref. [1], and a slightly larger cubic volume of 8 nm × 8 nm × 8 nm containing 16936 water molecules. For the sake of simplicity, only the OPLS + SPC/E force field was considered.

The radius of gyration R_g of the 30mer-PNIPAM chain was calculated to distinguish quantitatively between the collapsed and the stretched state. As in Ref. [1], the 30mer-PNIPAM chain was considered collapsed when R_g is below the threshold of 1.25 nm. A radius of gyration between 0.95 to 1.30 nm has been reported for the 30mer-PNIPAM chain in the collapsed state by Boţan *et al.* [12].

1.1 *Results for the small simulation volume*

To illustrate the head-tail artifact, we carried out the simulations using the same simulation volume employed by Walter *et al. [1]*. The temperature was set to 280 K and 300 K, respectively, which are both below the lower critical solution temperature (LCST) of PNIPAM. The initial radius of gyration of the 30mer-PNIPAM chain was 1.95 nm, i.e., it was initially in the stretched state.

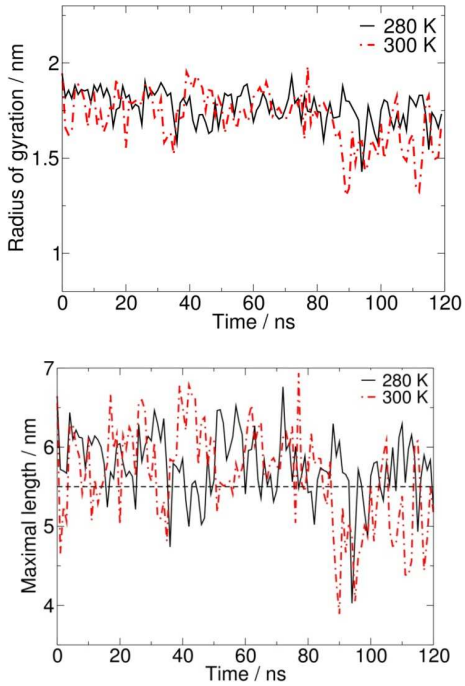

Figure S1. Simulation results in the small volume at 280 K and 300 K. (Top) Radius of gyration of the 30mer-PNIPAM as a function of time, and (bottom) maximal length of the 30mer-PNIPAM chain as a function of time. The dashed line is the length of the simulation volume in the in *y* and *z* directions minus the cutoff radius.

In the small volume, the 30mer-PNIPAM chain remains stretched during the entire simulation time (Figure S1 top), which is in agreement with the simulation results of Ref. [1]. For these simulations, the maximal distance between two atoms in the 30mer-PNIPAM chain reaches values that are larger than the length of the simulation volume in the *y* and *z* directions (7 nm) minus the cutoff radius (Figure S1 bottom). In the initial state, in which the polymer chain is placed along the *z* direction of the volume (9 nm), head and tail of the 30mer-

PNIPAM chain do not interact through the periodic boundary conditions. But as the polymer rotates, such head-to-tail interactions do occur because the extension of the volume on its shorter sides is only 7 nm and the cut-off radius is 1.5 nm. This artifact influences the simulation results. It is shown below that the head-tail interactions stabilize the stretched configuration so that these simulations cannot be used to study the coil-to-globule transition of PNIPAM.

1.2 *Results for the large simulation volume*

To avoid head-tail interactions, we carried out simulations using a slightly larger simulation volume than that employed in Ref. [1]. The dimensions of the simulation volume were 8 nm × 8 nm × 8 nm, which is large enough to avoid head-tail interactions (see Figure S2) . Three different initial configurations of the 30mer-PNIPAM chain were used: a stretched state (R_g = 1.95 nm), an intermediate state (R_g = 1.6 nm), and a close-to-collapsed state (R_g = 1.4 nm).

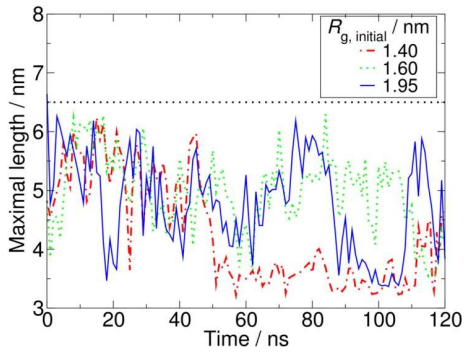

Figure S2. Maximal length of the 30mer-PNIPAM chain as a function of time using the large simulation volume at 300K. The dashed line is the length of the simulation volume in the in *y* and *z* directions minus the cutoff radius.

In the absence of head-tail interactions, the chain showed substantial fluctuations in the radius of gyration for all simulations (Figure S3). In no case, there was evidence for the

prevalence of the stretched configuration. Thus, no statement can be made about the equilibrium state of the 30mer-PNIPAM chain even though the simulation time was three times longer than in Ref. [1]. These results indicate that a much longer simulation time would be needed to sample the phase space in a sufficiently exhaustive manner.

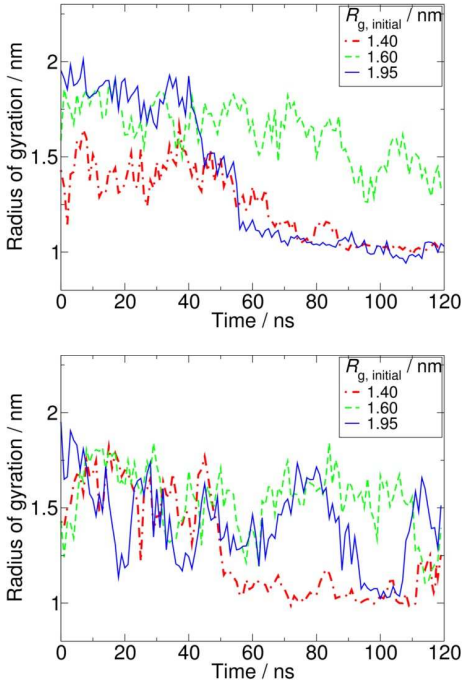

Figure S3. Radius of gyration of a 30mer-PNIPAM chain in water as a function of time: 280 K (top) and 300 K (bottom).

For monitoring convergence, the corrected Gelman-Rubin test [13] was carried out for the simulations in the large volume. The radius of gyration as a function of time obtained by these simulations using different starting configurations of the 30mer-PNIPAM chain was used as independent sequences. According to the Gelman-Rubin convergence test, adequate sampling is achieved when the mixture-of-sequences variance *V* and the within-sequence variance *W*

reach the same stationary value. Figure S4 shows that convergence was not reached within the simulation time (120 ns).

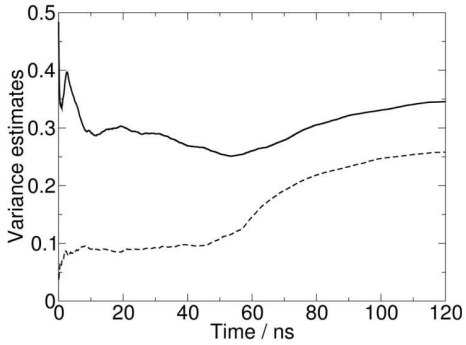

Figure S4. Corrected Gelman-Rubin convergence test [13] for three independent simulations of a 30mer-PNIPAM chain in water at 280 K. Mixture-of-sequences variance *V* (solid line) and within-sequence variance *W* (dashed line).

The lack of adequate sampling of the phase space thus does not allow drawing conclusions on the equilibrium state of the 30mer-PNIPAM chain from direct MD simulations even for a simulation time of 120 ns.

1.3 *Conclusions*

The simulation method used in Ref. [1] for studying the transition of PNIPAM is inappropriate for two reasons: (1) head-tail interactions occurred that artificially favored the stretched configuration, and (2) the sampling of the phase space was insufficient. Therefore, the conclusions on the equilibrium properties of PNIPAM presented in Ref. [1] are not well-founded. The simulation times presently attainable in direct MD simulations are probably insufficient for drawing conclusions on the equilibrium properties of the studied systems. More efficient simulation methods are needed to overcome this sampling problem. Such work is presently in progress in our group.

The same criticism as discussed here also applies to a related paper on cononsolvency of PNIPAM in water/methanol mixtures.[14] However, the qualitative explanation given in that paper for the cononsolvency effect is still valid.

2. Simulations using the two periodic molecules scenario.

2.1 *Force field*

Figure S5 and Table S1 present the force field used in the present work to describe the polymer molecules.

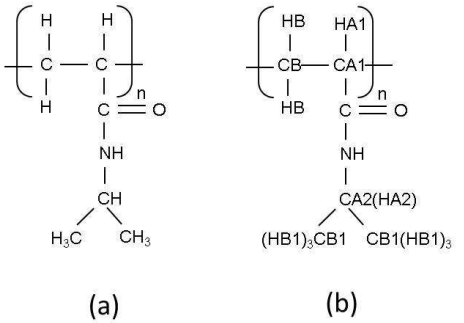

Figure S5. (a) PNIPAM molecule (b) PNIPAM molecule with the name of the atoms used in the force field.

Table S1. OPLS-AA parameters

Atom	Gromacs opls code	Charge / e	σ / nm	ε / kJ/mol
CB	opls_136	-0.120	0.350	0.276144
HB	opls_140	0.060	0.250	0.125520
CA1	opls_137	-0.060	0.350	0.276144
HA1	opls_140	0.060	0.250	0.125520
C	opls_235	0.500	0.375	0.439320
O	opls_236	-0.500	0.296	0.878640
N	opls_238	-0.500	0.325	0.711280
H	opls_241	0.300	0.000	0.000000
CA2	opls_224B	0.140	0.350	0.276144
HA2	opls_140	0.060	0.250	0.125520
CB1	opls_135	-0.180	0.350	0.276144
HB1	opls_140	0.060	0.250	0.125520

Figure S6 shows the potential of means force $G(d)$ for different temperature for $\xi = 1.0$. The chains tend to form an aggregated state at low temperature. The tendency to form an aggregated state configuration increases with the temperatures. This indicates that the transition between the aggregated and the dissolved state occurs at lower temperature than 280 K, which is way below the LCST of PNIPAM. Therefore, the unmodified OPLS + SPCE force field is unable to reproduce such transition.

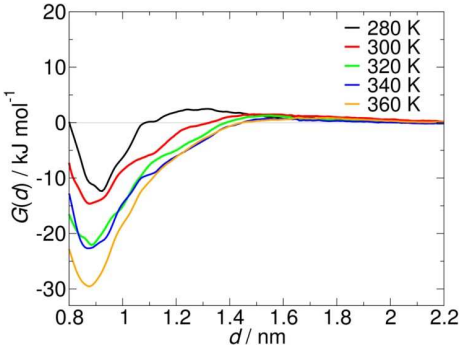

Figure S6. PMF profiles calculated using the unmodified water-polymer mixing rule (ξ = 1.0).

Figure S7 show an example of umbrella histogram. It can be seen that successive windows significantly overlap.

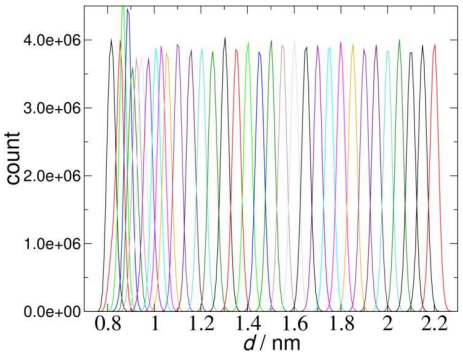

Figure S7. Histograms in umbrella sampling at 280 K for $\xi = 1.15$.

2.2 *Convergence of the PMF with simulation time*

The potential of mean force $G(d)$ was calculated using different total simulation times. There is no significant change in the PMF after 816 ns. This simulation time is divided into 34 umbrella windows.

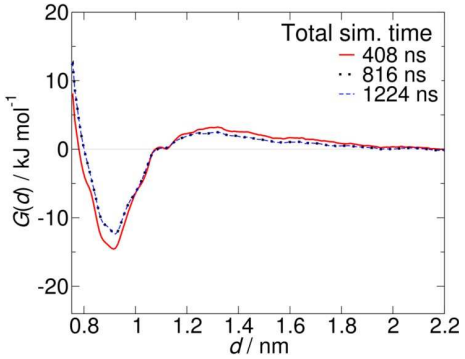

Figure S8. PMF at 280 K for several total simulation times for $\xi = 1.0$

2.3 *Effect of the size of the simulation box*

To determine whether the simulations with the two periodic molecules scenario are free of finite-size effects, we studied the influence of the number of water molecules in the simulation box on the PMF. A series of umbrella sampling simulations were carried out using different numbers of water molecules for the modified mixing rule with $\xi = 1.15$. The number of water molecules was systematically changed by increasing the initial size of the simulation box in the *y* and *x* directions. For the sake of simplicity, the length of the box in the *x*- and *y*-direction was set to the same value. The number of monomers per chain was 15, and the initial length of the box in the *z* direction was determined by the length of the relaxed chain. Table S2 gives the number of water molecules for the corresponding initial size of the box.

Table S2. Initial dimensions of the simulation box used for studying the effect of the number of water molecules on $G(d)$. The number of monomers in each PNIPAM molecules was 15.

Box dimensions (x, y, z) / nm	Number of water molecules
5.0 x 5.0 x 3.785	2883
6.0 x 6.0 x 3.785	4227
7.0 x 7.0 x 3.785	5835

When the initial size of the simulation box is larger or equal to 5 nm, no finite-size effect is observed on the values on the PMF (Figure S9). The small deviation in the $G(d)$ using the box size of 5.0, 6.0, and 7.0 nm are within the statistical uncertainty.

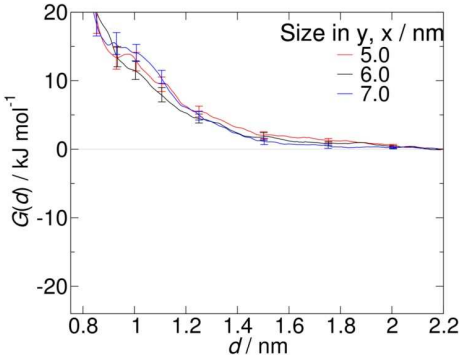

Figure S9. PMF at 280 K for several sizes of the simulation box in the *x* and *y* directions. The *z* direction was kept fixed to maintain the length of the periodic molecule at 15 monomers per chain. $\xi = 1.15$ was used.

2.4 *Effect of the number of monomers in the PNIPAM chain*

Figure S10 shows the potential of mean force $G(d)$ for different lengths of the polymer chains for $\xi = 1.15$. As the number of monomers per chain increases, $G(d)$ raises for $G(d) > 0$ at low temperature whereas it decreases $G(d) < 0$ at high temperatures. However, the position of the minimum of $G(d)$ at about $d = 0$ nm is not affected by the number of monomers.

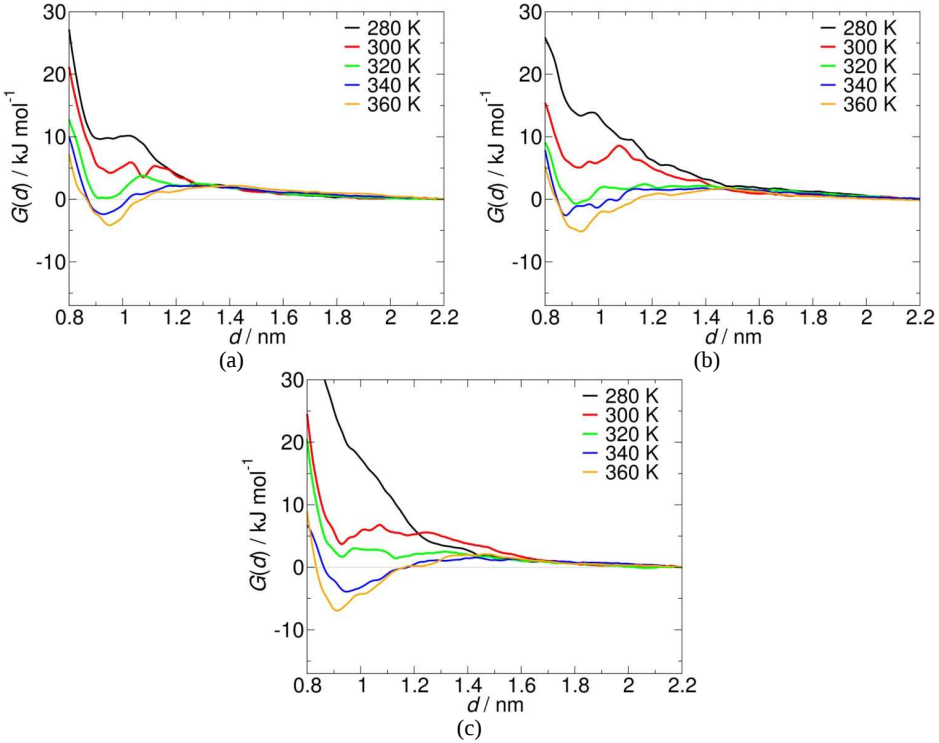

Figure S10. Potential of mean force $G(d)$ using ξ = 1.15 for several numbers of monomer per PNIPAM chain: (a) 12, (b) 15, and (c) 18.

Figure S11 shows $\Delta G_{d\to a}$ as a function of the temperature for different lengths of the polymer chain, and Table S3 give the thermodynamic properties obtained by fitting such data. Similar transition temperatures are obtained for 15 and 18 monomers per chain. As the number of monomers per chain increases, the additional polymer-polymer repulsion at low temperature is compensated by the additional polymer-polymer attraction at high temperature.

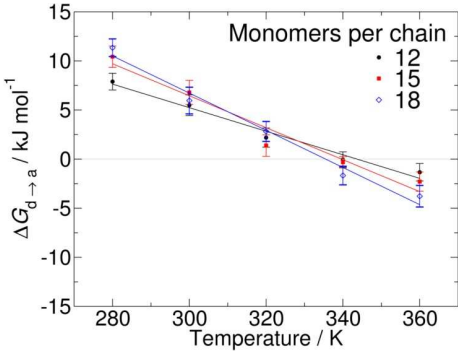

Figure S11. Free energy of the transition from the dissolved to the aggregated state as a function of the temperature for ξ = 1.15 using different lengths of the polymer chain.

Table S3. Thermodynamic properties of the coil-globule transition.

Property / monomers per chain	12	15	18
T_θ / K	343 ± 10	339 ± 14	335 ± 9
$\Delta H_{d\to a}$ / kJ/mol per monomer	1.7 ± 0.1	1.8 ± 0.1	1.8 ± 0.1
$\Delta S_{d\to a}$ / J/K/mol per monomer	5.0 ± 0.1	5.4 ± 0.1	5.2 ± 0.1

References

[1] J. Walter, V. Ermatchkov, J. Vrabec, H. Hasse, Molecular dynamics and experimental study of conformation change of poly(N-isopropylacrylamide) hydrogels in water, Fluid Phase Equilibria. 296 (2010) 164–172. doi:10.1016/j.fluid.2010.03.025.

[2] W.F. van Gunsteren, J.C. Berendsen, Groningen Molecular Simulation (GROMOS) Library Manual, Biomos, Groningen, The Netherlands, 1987.

[3] C. Oostenbrink, A. Villa, A.E. Mark, W.F. van Gunsteren, A biomolecular force field based on the free enthalpy of hydration and solvation: the GROMOS force-field parameter sets 53A5 and 53A6, J. Comput. Chem. 25 (2004) 1656–1676. doi:10.1002/jcc.20090.

[4] C. Oostenbrink, T.A. Soares, N.F.A. van der Vegt, W.F. van Gunsteren, Validation of the 53A6 GROMOS force field, Eur. Biophys. J. EBJ. 34 (2005) 273–284. doi:10.1007/s00249-004-0448-6.

[5] W.L. Jorgensen, D.S. Maxwell, J. Tirado-Rives, Development and testing of the OPLS All-Atom force field on conformational energetics and properties of organic liquids, J. Am. Chem. Soc. 118 (1996) 11225–11236. doi:10.1021/ja9621760.

[6] W.L. Jorgensen, J. Tirado-Rives, The OPLS [optimized potentials for liquid simulations] potential functions for proteins, energy minimizations for crystals of cyclic peptides and crambin, J. Am. Chem. Soc. 110 (1988) 1657–1666. doi:10.1021/ja00214a001.

[7] H.J.C. Berendsen, J.R. Grigera, T.P. Straatsma, The missing term in effective pair potentials, J. Phys. Chem. 91 (1987) 6269–6271. doi:10.1021/j100308a038.

[8] W.L. Jorgensen, J. Chandrasekhar, J.D. Madura, R.W. Impey, M.L. Klein, Comparison of simple potential functions for simulating liquid water, J. Chem. Phys. 79 (1983) 926–935. doi:10.1063/1.445869.

[9] H. Du, R. Wickramasinghe, X. Qian, Effects of Salt on the Lower Critical Solution Temperature of Poly (N-Isopropylacrylamide), J. Phys. Chem. B. 114 (2010) 16594–16604. doi:10.1021/jp105652c.

[10] H. Du, S.R. Wickramasinghe, X. Qian, Specificity in cationic interaction with poly(N-isopropylacrylamide), J. Phys. Chem. B. 117 (2013) 5090–5101. doi:10.1021/jp401817h.

[11] S.A. Deshmukh, Z. Li, G. Kamath, K.J. Suthar, S.K.R.S. Sankaranarayanan, D.C. Mancini, Atomistic insights into solvation dynamics and conformational transformation in thermo-sensitive and non-thermo-sensitive oligomers, Polymer. 54 (2013) 210–222. doi:10.1016/j.polymer.2012.11.009.

[12] V. Boţan, V. Ustach, R. Faller, K. Leonhard, Direct phase equilibrium simulations of NIPAM oligomers in water, J. Phys. Chem. B. 120 (2016) 3434–3440. doi:10.1021/acs.jpcb.6b00228.

[13] S.P. Brooks, A. Gelman, General methods for monitoring convergence of iterative simulations, J. Comput. Graph. Stat. 7 (1998) 434–455. doi:10.1080/10618600.1998.10474787.

[14] J. Walter, J. Sehrt, J. Vrabec, H. Hasse, Molecular dynamics and experimental study of conformation change of poly(N-isopropylacrylamide) hydrogels in mixtures of water and methanol, J. Phys. Chem. B. 116 (2012) 5251–5259. doi:10.1021/jp212357n.